Peer-reviewed version available at Catalysts 2019, 9, 994; doi:10.3390/catal9120994

Catalytic combustion of dimethyl disulfide on bimetallic supported catalysts prepared by the wet-impregnation method

Junan Gao [1], Song Gao [1], Jun Wei [2], Hong Zhao [1], Jie Zhang [1,] *,

1 State Key Laboratory of Chemical Resource Engineering, Beijing University of Chemical Technology, Beijing 100029, China

2 Hangzhou Yinli Environmental Protection Technology Co., Ltd., Hangzhou 310016, China

* Correspondence: zhangjie@mail.buct.edu.cn; Tel.: +86-1800-113-7991

Abstract: In this paper, the catalytic combustion of DMDS (dimethyl disulfide, CH_3SSCH_3) over bimetallic supported catalysts were investigated. It was confirmed that Cu/γ-Al_2O_3-CeO_2 showed best catalytic performance among the five single-metal catalysts. Furthermore, six different metals were separately added into Cu/γ-Al_2O_3-CeO_2 to investigate the promoting effect. The experiments revealed Pt as the most effective promoter and the the best catalytic performance was achieved as the adding amount of 0.3 wt%. The characterization results indicated that high activity and resistance to sulfur poisoning of Cu-Pt/γ-Al_2O_3-CeO_2 could be attributed to the synergistic effect between Cu and Pt.

Keywords: Catalytic combustion; Dimethyl disulfide; Bimetallic; Supported catalyst

1. Introduction

Sulfur containing volatile organic compounds (SVOCs) emissions are exhaust gases containing organic sulfur compounds such as thiophene, mercaptans, and thioethers. Almost all hydrocarbons contain organic sulfur compounds in their raw materials, a large number of SVOCs will be produced in the process of dye manufacturing, pesticide production, coatings industry, leather production, landfill and wastewater treatment [1-3]. Some exhaust gases containing organic sulfur compounds can cause malodors and damage to skin and eyes even at low concentrations [4-7]. At present, there are many SVOCs treatment methods: condensation method, adsorption method, catalytic

combustion method, low temperature plasma purification method, biological method et al. [8-12]. Catalytic combustion SVOCs will produce CO_2, H_2O, SO_2 and other compounds, supplemented by an exhaust gas absorption device, which can completely eliminate SVOCs. It is a promising SVOCs treatment method. Because DMDS (dimethyl disulfide, CH_3SSCH_3) is among the most odorous compounds due to its low human detection threshold (2.5 μg/m^3), which makes it rather difficult to treat completely [13-15], DMDS was selected reactant of this study.

There are many supports for catalytic combustion of DMDS：γ-Al_2O_3，CeO_2，SiO_2，TiO_2, ZrO_2, ZSM-5 [16-18]. These supports with a high specific surface area increase the dispersibility of the metal, the adsorption capacity of the reactants, and the reduction of the loading of the metal [19, 20]. γ-Al_2O_3 and CeO_2 has been the most widely studied and applied due to its high specific surface area, stability and low price [21]. Therefore, this study used two supports, CeO_2 and γ-Al_2O_3, for experiments. The support γ-Al_2O_3, CeO_2, γ-Al_2O_3-CeO_2 alone has almost no catalytic activity. So the catalysts that are commonly used for DMDS catalytic combustion are supported noble metals, transition metal oxides and bimetallic oxides catalysts [23-25]. Noble metal supported catalysts have long been considered to be the desirable catalyst for catalytic combustion of SVOCs due to their higher specific activity, resistance to deactivation and regenerability [26-28]. However, Pt, Pd, and Au-based catalysts are limited in their application in dealing with organic chlorine and organic sulfur exhaust gas due to high price and poor resistance to sulfur poisoning. More and more researchers are working on the catalytic combustion of DMDS in transition metal catalysts to explore highly efficient and stable transition metal catalysts, replacing noble metal catalysts [29]. Oxides of transition metals, mainly Mn, Co, Fe and Cu are employed for the combustion of DMDS [30].

At present, there are many studies on catalysts for catalytic combustion of DMDS, but problems such as poor activity, sulfur poisoning, and poor selectivity of SO_2 are common. In the process of catalytic combustion of DMDS, sulfur compounds bond tightly to the active site of the catalyst forming stable surface metal sulfides, which prevent adsorption of reactants on the surface [31]. Sulfur can also concentrate on the oxide support forming sulfates such as aluminum sulfates and cerium oxy-sulfates, which

can have an impact on the metal-support interaction.

In this study, the support of catalyst was screened firstly. Then the most active of the several γ-Al_2O_3-CeO_2 supported single-metal oxides was determined as the principal catalyst. A variety of metal oxides were separately added to this catalyst to investigate the promoting effect, and the most effective one was selected as a promoter in later investigation. The physicochemical properties of the catalyst and its structure-activity relationship were studied by using characterization techniques. Finally, the effects of catalyst preparation conditions on the catalytic activity of Cu-Pt/γ-Al_2O_3-CeO_2 catalystic combustion DMDS were investigated, and long-term stability experiments were performed.

2. Results and Discussion

2.1. Effect of the supports

In order to study the effect of different supports on the activity of supported catalysts，Cu/(γ-Al_2O_3, CeO_2, γ-Al_2O_3-CeO_2) and Cu-Pt/(γ-Al_2O_3, CeO_2, γ-Al_2O_3-CeO_2) catalysts were prepared, the performance of catalytic combustion DMDS were investigated，and the results are shown in Fig. 1. Under the experimental conditions, the DMDS catalytic ignition temperatures of Cu/γ-Al_2O_3-CeO_2, Cu/γ-Al_2O_3 and Cu/CeO_2 catalysts are 200 ºC-300 ºC. The catalytic activity of DMDS is compared between three Cu-based catalysts and the order of activity: Cu/γ-Al_2O_3-CeO_2>Cu/γ-Al_2O_3>Cu/CeO_2. Moreover, it can be seen that the activity of Pt-Cu bimetallic supported catalyst is consistent with that of Cu single-metal supported catalyst. The catalytic activity of Cu-Pt/γ-Al_2O_3-CeO_2 catalyst is significantly higher than that of Cu-Pt/γ-Al_2O_3 and Cu-Pt/CeO_2. Compared with γ-Al_2O_3, γ-Al_2O_3-CeO_2 has great advantages in catalytic combustion of DMDS for the addition of CeO_2. Because CeO_2 has a very strong oxygen storage capacity, and the transfer of charge between the active species and the CeO_2 support is beneficial to enhance the reactivity of the catalyst. Therefore, γ-Al_2O_3-CeO_2 was chosen as the catalyst support in this study.

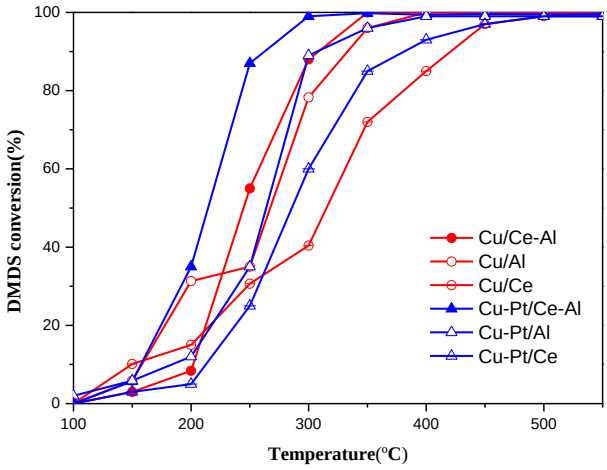

Fig.1. Activity diagram of catalytic combustion of DMDS by Cu/(γ-Al_2O_3, CeO_2, γ-Al_2O_3-CeO_2) and Cu-Pt/(γ-Al_2O_3, CeO_2, γ-Al_2O_3-CeO_2) catalysts. Al is γ-Al_2O_3, Ce is CeO_2, and Ce-Al is γ-Al_2O_3-CeO_2, which is the same as the following figure.

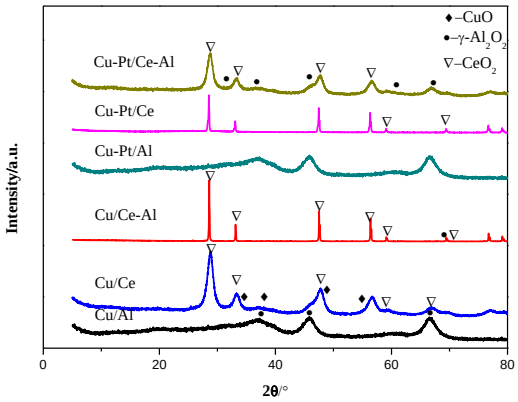

Fig. 2. XRD patterns of Cu/(γ-Al_2O_3, CeO_2, γ-Al_2O_3-CeO_2) and Cu-Pt/(γ-Al_2O_3, CeO_2, γ-Al_2O_3-CeO_2) catalysts

The XRD patterns of Cu/(γ-Al_2O_3, CeO_2, γ-Al_2O_3-CeO_2) and Cu-Pt/(γ-Al_2O_3, CeO_2, γ-Al_2O_3-CeO_2) catalysts are showed in Fig.2, in which we can observe the dispersibility of the active component on the support from a microscopic point of view. The diffraction

peak of CuO on the Cu/CeO_2 catalyst can be clearly observed, indicating that the Cu phase on the surface of the CeO_2 support is in the form of larger CuO, which is more unfavorable for the catalytic combustion reaction. Therefore, CeO_2 supported single-metal catalysts have the worst activity. With no diffraction peaks of CuO appearing in the Cu-Pt/CeO_2 catalyst, it can be inferred that the addition of Pt causes CuO to form smaller particle grains and improve the distribution of CuO. In addition, comparing with the Cu/γ-Al_2O_3-CeO_2 and Cu/γ-Al_2O_3 XRD patterns, it was found that the addition of CeO_2 enhanced the regularity of the Al_2O_3 micropores and facilitated the dispersion of CuO. The XRD patterns of Cu-Pt/(γ-Al_2O_3, CeO_2, γ-Al_2O_3-CeO_2) do not show the diffraction peaks of Cu phase or Pt phase. It can be inferred that Cu phase or Pt phase in support are present in the form of oxides of highly dispersed small particles, which is advantageous for the reaction [33].

3.2. Single-metal supported catalyst

In order to select the principal catalyst, activity of single-metal supported catalyst was evaluated, and the characteristic temperature diagram of catalytic combustion of DMDS of (Cu, Fe, Zn, Mo, V)/γ-Al_2O_3-CeO_2 catalyst are showed in Fig.3. The complete conversion temperature of Cu/γ-Al_2O_3-CeO_2 is about 308°C, which is obviously superior to other catalysts. The complete conversion temperature of V/γ-Al_2O_3-CeO_2 and Zn/γ-Al_2O_3-CeO_2 catalysts is about 345°C, and the catalytic effect is not obvious. At the same time, T50 (temperature at which DMDS conversion rate is 50%) is the main evaluation condition, supplemented by T10 (temperature when DMDS conversion rate is 10%) and T90 (temperature when DMDS conversion rate is 90%). The DMDS catalytic activity of a transition metal catalyst is obtained in order of activity from high to low: (Cu>Fe>Mo>V>Zn)/γ-Al_2O_3-CeO_2. Based on the above analysis, the catalytic activity of Cu/γ-Al_2O_3-CeO_2 catalyst for oxidizing DMDS is the highest in the transition metal

supported γ-Al_2O_3-CeO_2 supported catalyst and was served as the principal catalyst for further investigation.

Fig.4 shows the XRD patterns of (Cu, Fe, Zn, Mo, V)/γ-Al_2O_3-CeO_2 catalyst, in which we can know the effect of the dispersibility of the active component on the catalytic activity. It can be found that after metal supported such as Cu, Fe, Zn, Mo and V, the diffraction peak of the support spectrum is clearly visible, and the position of the peak does not change, indicating that the support retains the mesoporous structure intact after metal ion impregnation [34,35]. Only ZnO is present in the form of large particles on the support, which diffraction peaks are clearly visible, so its catalytic combustion activity is lowest. The intensity of diffraction peaks of (Fe, Zn, Mo, V)/γ-Al_2O_3-CeO_2 catalysts is slightly decreased, and the intensity of Cu/γ-Al_2O_3-CeO_2 diffraction peaks is slightly increased, indicating that the Fe, Zn, Mo, and V metal loadings reduce the regularity of the mesopores, while the Cu loading increases the regularity of the mesopores [36].

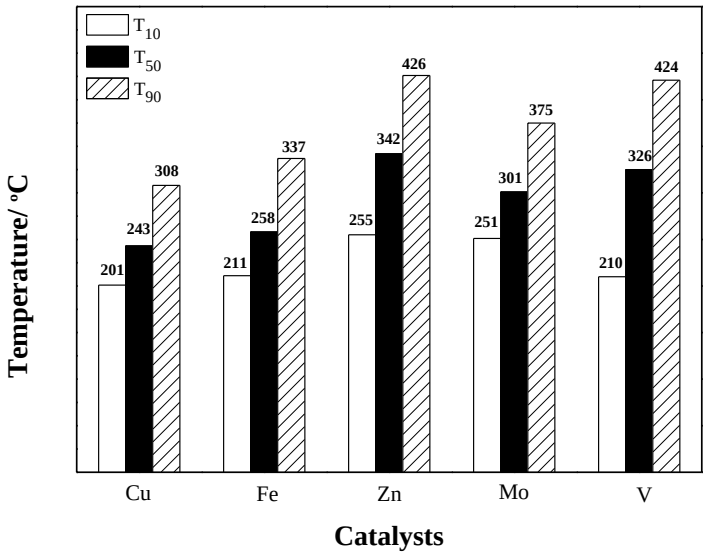

Fig.3. Characteristic temperature diagram of catalytic combustion of DMDS with （Cu, Fe, Zn, Mo, V)/γ-Al_2O_3-CeO_2 catalyst

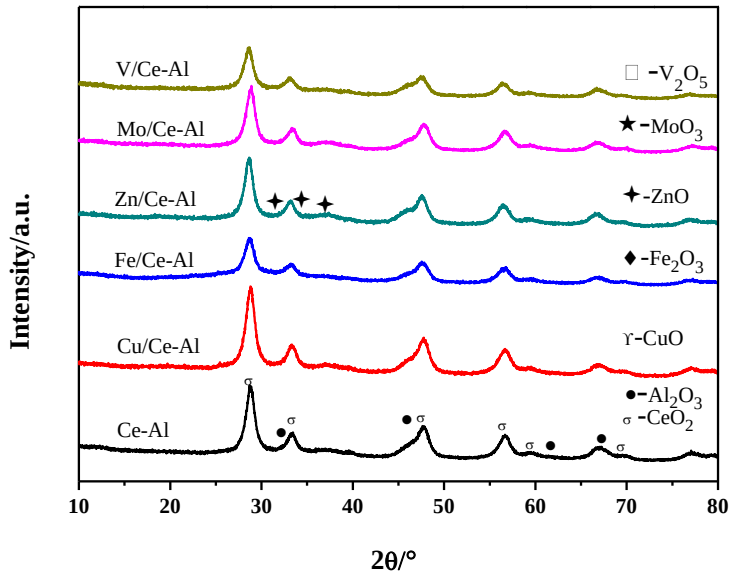

Fig.4. XRD spectrum of（Cu, Fe, Zn, Mo, V)/γ-Al_2O_3-CeO_2 catalyst

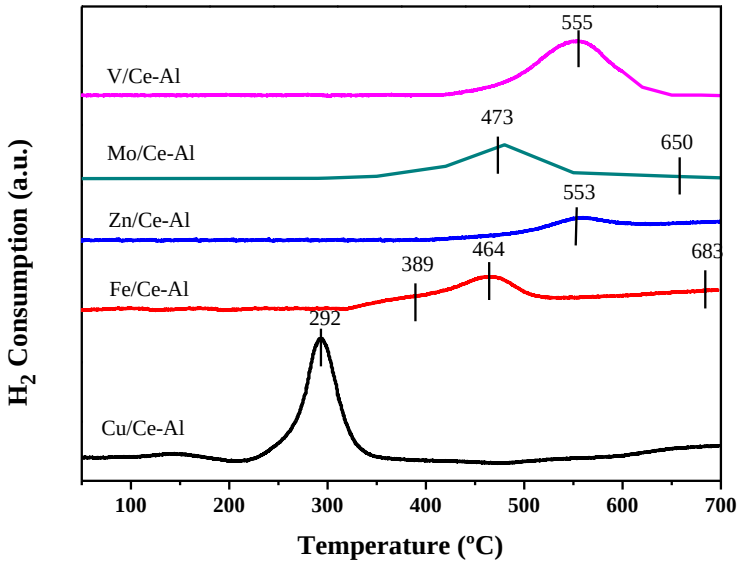

Fig .5. H_2-TPR spectrum of (Cu, Fe, Zn, Mo, V)/γ-Al_2O_3-CeO_2 catalyst

The TPR spectrum can effectively see the hydrogen consumption of the supported oxide reduction, the ease of reduction, and the interaction between the metal oxide and the support. The H_2-TPR spectrum of the (Cu, Fe, Zn, Mo, V)/γ-Al_2O_3-CeO_2 catalyst are showed in Fig.5. γ-Al_2O_3-CeO_2 catalyst showed a reduction peak at 294°C, which can be

attributed to CuO reduction [37]. By comparison, it was found that the reduction peak of Cu/γ-Al_2O_3-CeO_2 catalyst had the lowest temperature, the highest peak intensity and the best reduction. The redox capacities of the catalysts are ranked: （Cu>Fe>Mo>V>Zn）/γ-Al_2O_3-CeO_2, which is highly consistent with the catalytic combustion activity of the transition metal catalyst DMDS. It is inferred that the stronger the redox ability of the catalyst, the stronger the catalytic combustion activity of DMDS.

3.3. Bimetallic catalyst

Cu/γ-Al_2O_3-CeO_2 catalyst was determined as the principal catalyst, due to its low redox temperature and the best activity of catalytic combustion of DMDS in transition metals. A variety of metal oxides (Mo, Fe, Zn, V, Pt, Pd) were separately added to this catalyst to investigate the promoting effect. Fig.6 shows the characteristic temperature of catalytic combustion of DMDS by (Cu, Cu-Mo, Cu-Fe, Cu-Zn, Cu-V, Cu-Pt, Cu-Pd)/γ-Al_2O_3-CeO_2 catalysts. Compared with the catalytic activity of Cu/γ-Al_2O_3-CeO_2, when the promoter is a transition metal, it is found that Cu-Mo/γ-Al_2O_3-CeO_2 is superior to other catalysts, and T90 is about 285°C. The addition of Mo metal increased the catalytic activity of Cu/γ-Al_2O_3-CeO_2. After the addition of Zn and Fe, the catalytic activity of DMDS was not significantly improved, while the catalytic activity of Cu-V/γ-Al_2O_3-CeO_2 catalyst was 340°Cand T90 was about 449°C. It can be seen that the addition of V inhibits the catalytic activity of Cu/γ-Al_2O_3-CeO_2. When promoter was a noble metal, it was found that (Pt, Pd)/γ-Al_2O_3-CeO_2 had good activity for catalytic combustion of DMDS and Pt-Cu/γ-Al_2O_3-CeO_2 was more significant.

In order to evaluate the ability of catalyst to resist sulfur poisoning, the stability of DMDS for 48 h (Cu, Pt, Cu-Mo, Cu-Fe, Cu-Zn, Cu-V, Cu-Pt, Cu-Pd)/γ-Al_2O_3-CeO_2 catalysts are showed in Fig.7. The evaluation conditions were: GHSV (gaseous hourly space velocity) of 50000 h^{-1}, reaction temperature of 300°C, and DMDS concentration of 1000 ppm. The results show, the addition of （Mo，Pt，Pd） metal enhances the sulfur resistance of Cu/γ-Al_2O_3-CeO_2. But only Cu-Pt/γ-Al_2O_3-CeO_2 catalytic combustion DMDS activity is always maintained at about 100%, catalytic activity of

Pt/γ-Al_2O_3-CeO_2 is rapidly inactivated for poor resistance to sulfur poisoning. The reason for catalyst deactivation is that sulfur compounds bond tightly to the active site of the catalyst forming stable surface metal sulfides during catalytic combustion, which prevent adsorption of reactants on the surface [38-40]. It can be seen from Fig.10 that the Pt phsae in the Cu-Pt/CeO_2-Al_2O_3 catalyst exists in the form of Pt^0. The presence of Pt^0 can enhance the dispersibility, reduction and sulfur poisoning ability of CuO than PtO [41]. Combined with Fig.6, it is found that the catalytic activity of Cu-Pt/γ-Al_2O_3-CeO_2 catalyst DMDS is the highest, and the good sulfur poisoning ability. Cu-Pt/γ-Al_2O_3-CeO_2 catalyst is an ideal catalyst for catalytic combustion of DMDS.

Fig.8 shows the XRD patterns of (Cu, Cu-Mo, Cu-Fe, Cu-Zn, Cu-V, Cu-Pt, Cu-Pd)/γ-Al_2O_3-CeO_2 catalysts, in which we can obtain information of the structure or morphology of the molecules inside the material. Cu, Cu-Mo, Cu-Fe, Cu-Zn, Cu-V Cu-Pt, Cu-Pd supported on the γ-Al_2O_3-CeO_2 support, the diffraction peak of the γ-Al_2O_3-CeO_2 support spectrum is clearly visible, and the position of the peak does not change [42]. It indicates that the support retains its structure intact after metal ion impregnation. However, after the addition of Fe, Zn, Mo, V, Pt and Pd, the intensity of the diffraction peak of the bimetallic catalyst is lower than that of the Cu/γ-Al_2O_3-CeO_2 catalyst. It indicates that the addition of Fe, Zn, Mo, V, Pt and Pd changes the regularity of Cu/γ-Al_2O_3-CeO_2 mesopores and reduces the crystallinity of γ-Al_2O_3-CeO_2. Only the characteristic diffraction peaks of Cu-Zn/γ-Al_2O_3-CeO_2 catalysts are observed, which catalytic activity and sulfur poisoning ability are not good, other metal oxide characteristic peaks are not found. This may be because the impregnation process and the calcination process are good for the catalyst treatment and the Cu, Fe, Mo, V, Pt and Pd phase have small particle size and are highly dispersed [43].

In order to obtain the information on the interaction between metal oxides or metal oxides and supports during the reduction process of supported metal catalysts, H_2-TPR spectrum of (Cu, Cu-Mo, Cu-Fe, Cu-Zn, Cu-V, Cu-Pt, Cu-Pd)/γ-Al_2O_3-CeO_2 catalysts are showed in Fig.9. It is found that the reduction peak of Cu-Pd/γ-Al_2O_3-CeO_2 catalyst at 166°C is attributed to the highly dispersed PdO, and there is a significant reduction peak at 271°C, which belongs to the reduction of CuO and the small particles of CeO_2 with

highly dispersed catalyst surface reduction [44]. The loading of Pt reduced the temperature of Cu/γ-Al_2O_3-CeO_2 support reduction, enhanced the strength of the reduction peak and enhanced its reducibility. This indicates that the effect of Pt on the surface of Cu-Pt/γ-Al_2O_3-CeO_2 on the reduction of CeO_2 is affected by CeO_2 hydrogen spillover effect [45]. The loading of Mo, Fe and Zn metals enhances the strength of the reduction peak of Cu-M/γ-Al_2O_3-CeO_2 catalyst, and the loading of V greatly reduces the reducibility of Cu-V/γ-Al_2O_3-CeO_2 catalyst.

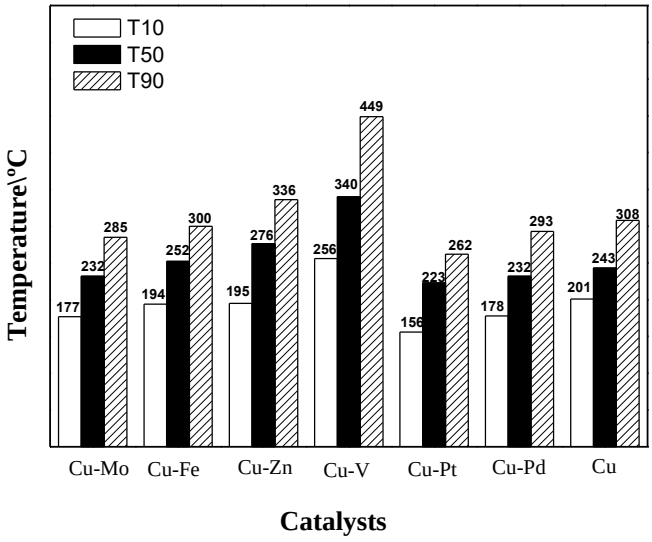

Fig.6. catalytic combustion temperature of DMDS of (Cu, Cu-Mo, Cu-Fe, Cu-Zn, Cu-V, Cu-Pt, Cu-Pd)/γ-Al_2O_3-CeO_2 catalysts

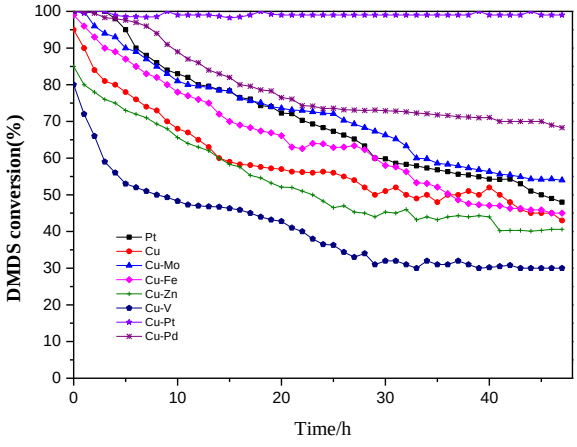

Fig. 7 (Cu, Cu-Mo, Cu-Fe, Cu-Zn, Cu-V, Cu-Pt, Cu-Pd)/CeO_2-Al_2O_3 catalysts for catalytic combustion of DMDS 48h stability diagram

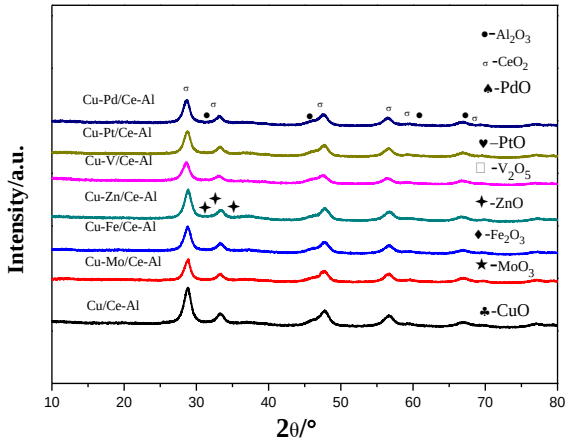

Fig.8. XRD patterns of (Cu, Cu-Mo, Cu-Fe, Cu-Zn, Cu-V, Cu-Pt, Cu-Pd)/γ-Al_2O_3-CeO_2 catalysts

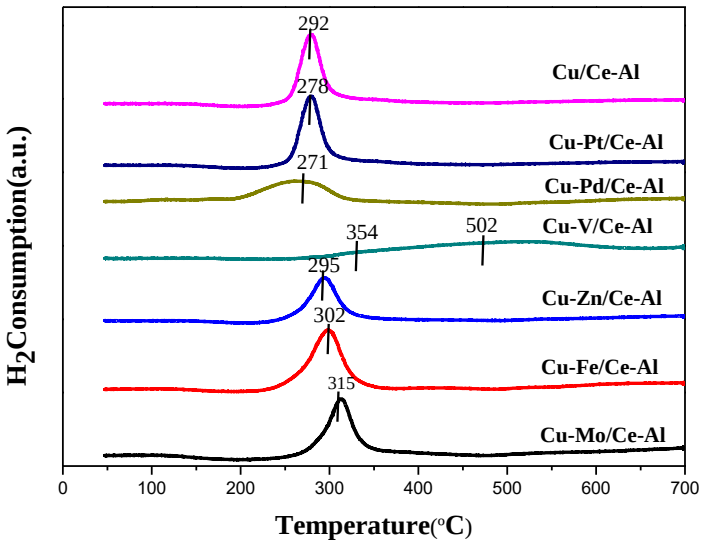

Fig.9. H_2-TPR diagram of (Cu, Cu-Pd, Cu-Pt, Cu-Mo, Cu-Fe, Cu-Zn, Cu-V)/γ-Al_2O_3-CeO_2 catalyst

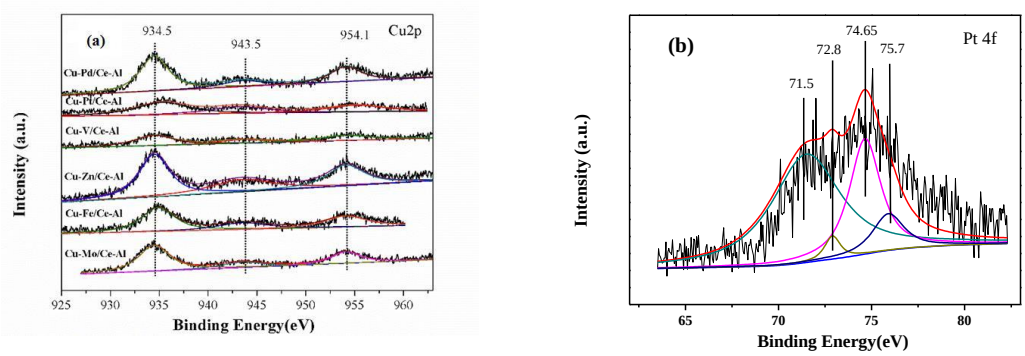

Fig.10. （a）Catalyst Cu2p of（Cu-Pd，Cu-Pt，Cu-Mo，Cu-Fe，Cu-Zn，Cu-V，Cu)/γ-Al_2O_3-CeO_2 （b） Pt4f XPS spectrum of Cu-Pt/γ-Al_2O_3-CeO_2

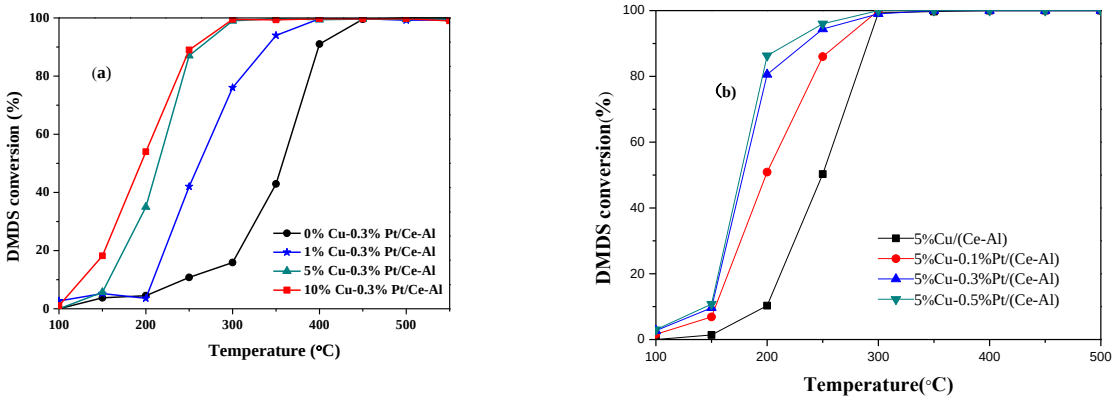

Fig.11. （a）Activity diagram of catalytic combustion of DMDS by (0%,1%,5%,10%)Cu-0.3%Pt/γ-Al_2O_3-CeO_2，（b）Activity diagram of catalytic combustion of DMDS by 5%Cu-（0%,0.1%,0.3%,0.5%）Pt/γ-Al_2O_3-CeO_2

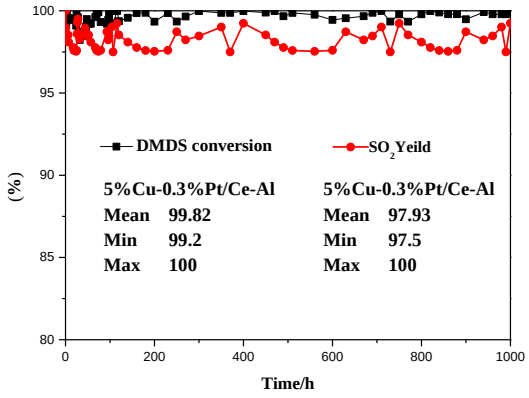

Fig.12. Catalytic combustion of DMDS with Cu-Pt/γ-Al_2O_3-CeO_2 catalyst for 1000h stability. Experimental condition: airspeed is 50000 h^{-1}, reaction temperature 300°C, DMDS concentration 1000 ppm, Oxygen concentration 5%.

In order to obtain the chemical and electronic states of the medium metal of the bimetallic catalyst, Cu2p of (Cu-Pd, Cu-Pt, Cu-Mo, Cu-Fe, Cu-Zn, Cu-V, Cu)/γ-Al_2O_3-CeO_2 catalyst are showed in Fig.10（a）. By comparison, it can be found that all the catalysts have three peaks, the main peak at BE=934.5 eV, corresponding to the characteristic peak of $Cu2p_{2/3}$ orbital. The satellite peaks at BE=943.5 eV and BE=954.1 eV belong to the characteristic peak of $Cu2p_{1/2}$, and there is no peak shift. The above information indicates that Cu phase on the surface of (Cu-Pd, Cu-Pt, Cu-Mo, Cu-Fe, Cu-Zn, Cu-V, Cu) /γ-Al_2O_3-CeO_2 catalysts mainly exist in the form of CuO [46]. Fig.10（b） shows XPS spectrum of a Cu-Pt/γ-Al_2O_3-CeO_2 catalyst. It can be found that the peaks of Cu-Pt/γ-Al_2O_3-CeO_2 catalyst Pt 4f at BE=71.2 eV and BE=74.65 eV are Pt $4f_{7/2}$ and Pt $4f_{5/2}$, respectively, which can be attributed to Pt^0 [47]. The shoulder peak at BE =72.8 eV can be attributed to PtO on the surface of the catalyst.

The right amount of loading is critical to the impact of the supported catalyst, so Fig.11 shows the catalytic combustion activity of DMDS for different loadings of Cu-Pt/γ-Al_2O_3-CeO_2 catalyst. It can be seen from the Fig.11 (a) that as the Cu loading increases from 0% to 10%, the DMDS catalytic combustion activity of the Cu catalyst gradually increases. As the Cu loading increases, the trend of catalyst activity growth decreases. The possible reasons are as follows: the specificity of the specific surface area

of the catalyst carrier itself is fixed. At the beginning of increasing the loading of Cu, more active sites can be introduced, which is beneficial to increase the catalytic combustion activity of DMDS. However, when the dispersibility of Cu species reaches the threshold, increasing the loading of Cu, it is impossible to introduce more active sites, and the excessive Cu loading will cause the clustering effect of the metal, and the catalytic combustion activity of DMDS cannot be further improved. It can be seen from Fig.11 (b) that as the Pt loading increases from 0% to 0.5%, the DMDS catalytic combustion activity of the catalyst gradually increases. However, as the Pt loading was from 0.3% to 0.5%, there was almost no change in catalyst activity growth. In summary, when the loading amount of Cu is 5% and the loading amount of Pt is 0.3%, it is economical and efficient.

Since the above results indicate that the Cu-Pt/γ-Al_2O_3-CeO_2 catalyst performance is ideal, we conducted long-term stability experiments, and the stability diagram of catalytic combustion of DMDS for 1000 h is showed in Fig.12. It can be found that the Cu-Pt/γ-Al_2O_3-CeO_2 catalyst maintains a DMDS conversion rate of about 100% and a SO_2 yield of 97% at a space velocity of 30,000 h^{-1} for a test period of 1000 h. Cu-Pt/γ-Al_2O_3-CeO_2 catalyst catalyzed combustion of DMDS with good stability and sulfur poisoning resistance is an ideal catalyst for catalytic combustion of DMDS. The possible reason for excellent catalyst stability is the addition of Pt significantly improves the redox ability of Cu-based catalysts，because the adsorption of reactive molecules, the activation of C-H bonds, and the oxidation of SOx during the catalytic combustion of dimethyl disulfide required higher potential. The addition of Pt enabled the Cu-based catalyst to promote the dissociation of O_2 at a lower potential, resulting in free O required for SOx oxidation；Dimethyl disulfide was easily partially oxidized during catalytic combustion to form reactive intermediates such as CO and SOx, which were attached to the active site to poison the Pt-based catalyst as a catalyst [48-50]. However, the addition of Cu can significantly enhanced the desorption and oxidation of CO and SOx by the catalyst, so the catalytic and resistance sulfur poisoning ability of Cu-Pt supported catalyst is excellent by the synergistic effect.

3. Experimental

3.1. Catalyst preparation and materials

Dimethyl disulfide (analytical grade), was purchased from Macklin Chemical Company. Pseudo-boehmite ($AlOOH \cdot nH_2O$, n=0.5) and Cerium nitrate hexahydrate, used as a support precursor, was purchased from Zibo Qichuang Chemical Company (Zibo, China). Platinum nitrate, palladium nitrate, copper nitrate, iron nitrate, zinc nitrate, molybdenum nitrate, vanadium nitrate, used as load metal precursor，were purchased from Aladdin Chemical Company and analytical grade.

For the preliminary screening purpose, the catalysts were all prepared by the incipient wetnes impregnation method. Pseudo-boehmite, barium nitrate or a mixture of them was impregnated with the solution that was prepared by dissolving known amounts of metal salts in deionized water. The mixed solution was magnetically stirred at room temperature for 18 hours. The well-impregnated catalyst precursors was spin-dried using a rotary evaporator, dried in air at 120ºC for 24 h, calcined in the oven with the air supply at 550ºC for 4 h, and then ground into particles of 40-60 mesh. The mixture of pseudo-boehmite and barium nitrate was prepared according to γ-Al_2O_3:CeO_2=10:1 (molar ratio). The metal content in the supported single-metal oxide catalyst is 5 wt%, while each of the supported bimetallic oxides catalyst consists of 5 wt% of Cu and 0.3 wt% of other metals.

3.2. Evaluation of the catalysts

The catalytic activity evaluation process of catalytic combustion DMDS is as follows. First, 0.2 g of catalyst was charged in the middle of the fixed bed reactor (quartz tube reactor with a diameter of 6.0 mm). Then, saturated steam of DMDS was introduced into the main line by nitrogen bubbling, and mixed with nitrogen and air. Finally, combustion reaction takes place in the fixed bed reactor. The reaction conditions are as follows: DMDS concentration is 1000 ppm, GHSV is 50000 h^{-1}, oxygen content is 5%, control temperature is raised from 100ºC to 550ºC, and stable at 5ºC for 20 minutes. The DMDS and concertration is detectedby gas chromatograph (Varian CP-3900, FID detector, OV-101 capillary column). The concertration of SO_2 was detected by flue gas

Peer-reviewed version available at Catalysts 2019, 9, 994; doi:10.3390/catal9120994

analyzer (Testo 350)

The conversion of DMDS, and yields of SO_2 are defined in the following way:

$$DMDS\ Conversion(\%) = \frac{Ci\text{-}C0}{Ci} \times 100 \quad (1)$$

$$SO_2\ Yield(\%) = \frac{[SO_2]}{2xCi} \times 100 \quad (2)$$

where Ci is the initial feed concentration of DMDS (ppm), C_0 is the outlet concentration of DMDS (ppm) and $[SO_2]$ is the concentrations of the corresponding compounds in mol·L^{-1}.

3.3. Catalyst characterization

The crystal structure analysis of the supported catalyst in this study was characterized by D8FOCUS X-ray diffractometer (XRD, Bruker, Germany). The diffractometer is equipped with CuKα rays, and the setting parameters are as follows: 2θ range 5–90°; step 0.1°and dwell time of 1 s. Diffraction patterns were compared to the ICDD database (International Center for Diffraction Data) for the identification of crystalline phases.

Characterization of supported catalyst surface used ESCALAB 250 X-ray photoelectron spectroscopy analyzer (XPS, Thermo Fisher, USA). The source is Al Kα, under ultra-high vacuum (UHV), with an X-ray current of 20 mA and a line voltage of 10 kV.

In this study, the oxidation/reduction performance of the catalyst was characterized by a TPR/D/O1100 catalyst fully automatic analyzer（Thermo Fisher Scientific）. The instrument is equipped with a highly sensitive TCD detector. The test procedure is as follows. First, 0.05 g of the catalyst sample is charged into the catalyst fully automatic analyzer for pretreatment. Pretreatment conditions: maintained at 200ºC for 1 h under a nitrogen atmosphere. Then cooled to room temperature and subjected to H_2 temperature programmed reduction. Test conditions: 5% (Vol.) H_2/N_2 flow rate 20 ml/min, temperature from 50 ºC to 700 ºC, heating rate 10 ºC/min.

4. Conclusion

γ-Al_2O_3-CeO_2 was observed to be the most optimal support and Cu was determined

as the principal active phase for catalytic combustion of DMDS. Among the six different types of biimetallic supported catalysts, the Cu-Pt/γ-Al_2O_3-CeO_2 catalyst exhibits the highest activity and sulfur poisoning ability for the DMDS combustion based on the conversion. According to XRD，H_2-TPR and XPS results, there are close interaction between Pt and Cu (intermetallic Pt-Cu) in the nano sized scale, which could be the main reason why this catalyst showed the highest activity.

Under the conditions of GHSV of 50000h^{-1}, DMDS concentration of 1000ppm and oxygen concentration of 5%, the prepared 5%Cu-0.3%Pt/γ-Al_2O_3-CeO_2 catalyst has the highest catalytic activity of DMDS, and 262ºCcan achieve complete conversion of DMDS. In addition, the 5%Cu-0.3%Pt/γ-Al_2O_3-CeO_2 catalyst has a conversion of about 100% in the 1000-hour stability test at a space velocity of 30000 h^{-1}, and the SO_2 yield is above 97%, which is an ideal catalyst for catalytic combustion of DMDS.

Author Contribution: Formal analysis and experiment, J.G.; writing—original draft preparation, S.G.; Investigation, J.W; writing—review and editing, H.Z.; funding acquisition and experimental design, J. Z.

Funding: This research was funded by Beijing science and technology projects Z181100005418011.

Conflicts of Interest: The authors declare no conflict of interest.

References

1. Aellach, B.; Ezzamarty, A.; Leglise, J.; Lamonier, C.; Lamonier, J.F. Calcium-Deficient and Stoichiometric Hydroxyapatites Promoted by Cobalt for the Catalytic Removal of Oxygenated Volatile Organic Compounds. *Catal. Lett.* **2010**, *135*, 197–206.
2. Faisal, I.; Khan, A.K. Removal of Volatile Organic Compounds from polluted air. *J. L. Pre.* **2000**, *13*, 527–545.
3. Lalanne. F.; Malhautier, L.; Roux, J.C. Absorption of a mixture of volatile organic compounds (VOCs) in aqueous solutions of soluble cutting oil. *Bio.Tech.* **2008**, *99*, 1699-1707.
4. Paloma, H.; Salvador, O.; Aurelio, V.; Fernando V.D. Catalytic combustion of methane over commercial catalystsin presence of ammonia and hydrogen sulphide. *Chemosphere.* **2004**, *55*,

681–689.

5. Wyrwalski, F.; Giraudon, J.M.; Lamonier, J.F. Synergistic Coupling of the Redox Properties of Supports and Cobalt Oxide Co_3O_4 for the Complete Oxidation of Volatile Organic Compounds *Catal. Lett.* **2010**, *137* , 141–149.
6. Hamad, A.; Fayed, M.E. Simulation-Aided Optimization of Volatile Organic Compounds Recovery Using Condensation. *Chem. Eng. Re & De.* **2004**, *82*, 895-906.
7. Azalim, S.; Franco, M.; Brahmi, R.; Giraudon, J.M.; Lamonier, J.F.; Hazard. J. Removal of oxygenated volatile organic compounds by catalytic oxidation over Zr–Ce–Mn catalysts. *Mater.* **2011**, *188*, 422–427.
8. Hongyan, P.; Mingyao, X.; Zhong, L.; Sisi, H.; Chun, H. Catalytic combustion of styrene over copper based catalyst: Inhibitory effect of water vapor. *Chemosphere.* **2009**, *76*, 721-726.
9. Spivey, J.J.; Butt, J.B .Literature review: deactivation of catalysts in the oxidation of volatile organic compounds. *Catal. Today.* **1992**, *11*, 465–500.
10. Nevanperä, T.K.; Ojala, S.; Bion, N. Catalytic oxidation of dimethyl disulfide (CH_3SSCH_3) over monometallic Au, Pt and Cu catalysts supported on γ-Al_2O_3, CeO_2 and CeO_2-Al_2O_3. *Appl.Catal. B* **2016**, *182*, 611-625.
11. Després, J.; Elsener, M.; Koebel, M. Catalytic oxidation of nitrogen monoxide over Pt/SiO_2. *Appl. Catal. B* **2004**, *50*, 73-82.
12. Galisteo, F.C.; Mariscal, R.; Granados, M.L.; Poves, Z.; Fierro, J.; Kröger, V.; Keiski, R.L. Reactivation of sulphated Pt/Al_2O_3 catalysts by reductive treatment in the simultaneous oxidation of CO and C_3H_6. *Appl. Catal. B* 2007, *72*, 272-281.
13. Halevi, B.; Vohs, J. M. Reactions of CH_3SH and $(CH_3)_2S_2$ on the (0001) and (000$\bar{1}$) Surfaces of ZnO. *J. Phy. Chem. B* **2005**, *109*, 23976-23982.
14. Kim, S.C.; Shim, W.G. Catalytic combustion of VOCs over a series of manganese oxide catalysts. *Appl. Catal. B* **2010**, *98*, 180–185.
15 Barakat, T.; Idakiev, V.; Cousin, R.; Shao, G.S.; Yuan, Z.Y. Total oxidation of toluene over noble metal based Ce, Fe and Ni doped titanium oxides. *Appl. Catal. B* **2014**, *146*, 138-146.
16 Tidahy, L.; Siffert, S.; Wyrwalski, F.; Lamonier, J.F.; Aboukaïs, A. Catalytic activity of copper and palladium based catalysts for toluene total oxidation. *Catal. Today.* **2007**, *119,* 317–320.
17. Yazawa, Y.; Takagi, N.; Yoshida, H. The support effect on propane combustion over platinum

catalyst: control of the oxidation-resistance of platinum by the acid strength of support materials. *Appl.Catal. A* **2002**, *233*, 103-112.

18. Lojewska, J.; Kolodziej, A.; Zak, J.; Stoch, J. Pd/Pt promoted Co_3O_4 catalysts for VOCs combustion: Preparation of active catalyst on metallic carrier. *Catal. Today.* **2005**, *105*, 655–661.
19. Beck, B.; Harth, M.; Hamilton, N.G. Partial oxidation of ethanol on vanadia catalysts on supporting oxides with different redox properties compared to propane. *J. Cat*. **2012**, *296*, 120-131.
20. Li, Y.; Yang, H.; Zhang, Y. Catalytic decomposition of HCN on copper manganese oxide at low temperatures: performance and mechanism. *J. Chem. Eng*. **2018**, *346*, 621-629.
21. Mishra, T.; Mahapatra, P.; Parida, K.M. Synthesis, characterisation and catalytic evaluation of iron–manganese mixed oxide pillared clay for VOC decomposition reaction. *Appl. Catal*. B **2008**, *79*, 279–285.
22. Ferrandon, M.; Carno, J.; Jaras, S.; Bjornbom, E. Total oxidation catalysts based on manganese or copper oxides and platinum or palladium I: Characterisation. *Appl. Catal. A* **1999**, *180*, 141–151.
23. Neyestanaki, A.K.; Klingstedt, F.; Salmi, T.; Murzin, D.Y. Deactivation of postcombustion catalysts, a review. *Fuel.* **2004**, *83*, 395-408.
24. Zhang J.; Cullen D.A; Forest R.V.; Wittkopf J.A.; Zhuang Z. Platinum–Ruthenium Nanotubes and Platinum–Ruthenium Coated Copper Nanowires As Efficient Catalysts for Electro-Oxidation of Methanol. *ACS Catal*. **2015**, *5*, 1468-1474.
25. Yige Zhao, Jingjun Liu, Chenguang Liu, Feng Wang, and Ye Song. Amorphous CuPt Alloy Nanotubes Induced by $Na_2S_2O_3$ as Efficient Catalysts for the Methanol Oxidation Reaction. *ACS Catal.* **2016**, *6*, 4127-4134.
26. Piumetti, M.; Andana, T.; Bensaid, S.; Fino, D.; Russo, N.; Pirone, R. Ceria-based nanomaterials as catalysts for CO oxidation and soot combustion, Effect of Zr-Pr doping and structural properties on the catalytic activity. *AIChE J*. **2016**, *63*, 216–225.
27. Rout, K.R.; Fenes, E.; Baidoo, M.F.; Abdollahi, R.; Fuglerud, T.; Chen, D. Highly Active and Stable CeO_2-Promoted $CuCl_2/Al_2O_3$ Oxychlorination Catalysts Developed by Rational Design Using a Rate Diagram of the Catalytic Cycle. *ACS Catal*. **2016**, *6*, 7030–7039.

28. Krishna, K.; Bueno-López, A.; Makkee, M.; Moulijn, J.A. Potential rare earth modifified CeO_2 catalysts for soot oxidation, I. Characterisation and catalytic activity with O_2. *Appl. Catal. B* **2007**, *75*, 189–200.
29. Eversfifield, P.; Liu, W.; Klemm, E. Effect of Potassium on the Physiochemical and Catalytic Characteristics of V_2O_5/TiO_2 Catalysts in o-Xylene Partial Oxidation to Phthalic Anhydride. *Catal. Lett.* **2017**, *147*, 785–791.
30. Weng, D.; Li, J.; Wu, X.; Si, Z. Modification of CeO_2-ZrO_2 catalyst by potassium for NOx-assisted soot oxidation. *J. Environ. Sci.* **2011**, *23*, 145–150.
31. Lu, C.; Liu, T.; Shi, Q.; Li, Q.; Xin, Y.; Zheng, L.; Zhang, Z. Plausibility of potassium ion-exchanged ZSM-5 as soot combustion catalysts. *Sci. Rep*. **2017**, *7*, 3300.
32. Lin, F.; Wu, X.; Weng, D. Effect of barium loading on CuOx–CeO_2 catalysts, NOx storage capacity, NO oxidation ability and soot oxidation activity. *Catal. Today*. **2011**, *175*, 124–132.
33. Weng, D.; Li, J.; Wu, X.; Si, Z. NOx-assisted soot oxidation over K/CuCe catalyst. *J. Rare Earth.* **2010**, *28*, 542–546.
34. Atribak, I.; Bueno-López, A.; Garcia-Garcia, A. Combined removal of diesel soot particulates and NOx over CeO_2–ZrO_2 mixed oxides. *J. Catal.* **2008**, *259*, 123–132.
35. Xiong, J.; Wu, Q.; Mei, X.; Liu, J.; Wei, Y.; Zhao, Z.; Wu, D.; Li, J. Fabrication of Spinel-Type $Pd_xCo_{3-x}O_4$ Binary Active Sites on 3D Ordered Meso-macroporous Ce-Zr-O_2 with Enhanced Activity for Catalytic Soot Oxidation. *ACS Catal*. **2018**, *8*, 7915–7930.
36. Liu, S.; Wu, X.; Lin, Y.; Li, M.; Weng, D. Active oxygen-assisted NO-NO_2 recycling and decomposition of surface oxygenated species on diesel soot with $Pt/Ce_{0.6}Zr_{0.4}O_2$ catalyst. *Chin. J. Catal*. **2014**, *35*, 407–415.
37. Yang, J.; Lukashuk, L.; Akbarzadeh, J.; Stöger-Pollach, M.; Peterlik, H.; Föttinger, K.; Rupprechter, G.; Schubert, U. Different synthesis protocols for Co_3O_4-CeO_2 catalysts-Part 1, influence on the morphology onthe nanoscale. *Chem. Eur. J.* **2015**, *21*, 885–892.
38. Zhou, R.; Guo, X. A new insight into the morphology effect of ceria on CuO/CeO_2 catalysts for CO selective oxidation in hydrogen-rich gas. *Catal. Sci. Technol*. **2016**, *6*, 3862–3871.
39. Konsolakis, M.; Carabineiro, S.A.C.; Marnellos, G.E.; Asad, M.F.; Soares, O.S.G.P.; Pereira, M.F.R.; Órfão, J.J.M.; Figueiredo, J.L. Volatile organic compounds abatement over copper-based catalysts, effect of support. *Inorg. Chim. Acta.* **2017**, *455*, 473–482.

40. Guan, B.; Lin, H.; Zhan, R.; Huang, Z. The catalysts of three-dimensionally ordered macroporous $Ce_{1-x}Zr_xO_2$-supported gold nanoparticles for soot combustion, The metal–support interaction. *J. Catal.* **2012**, *287*, 13–29.

41. Guan, B.; Lin, H.; Zhan, R.; Huang, Z. Catalytic combustion of soot over Cu, Mn substitution $CeZrO_{2-\delta}$, nanocomposites catalysts prepared by self-propagating high-temperature synthesis method. *Chem. Eng. Sci.* **2018**, *189*, 320–339.

42. Pfefferle, L.D.; Pfefferle, W.C. Catalysis in Combustion. *Catal. Rev. Sci. Eng.* **1987**, *29*, 219–267.

43. Kamal, M.S.; Razzak, S.A.; Hossain, M.M. Catalytic oxidation of volatile organic compounds (VOCs)—Areview. *Atmos. Environ.* **2016**, *140*, 117–134.

44. Zhang, Z.; Jiang, Z.; Shangguan, W. Low-temperature catalysis for VOCs removal in technology and application: A state-of-the-art review. *Catal. Today.* **2016**, *264*, 270–278.

45. Demoulin, O.; Clef, B.L.; Navez, M.; Ruiz, P. Combustion of methane, ethane and propane and of mixtures of methane with ethane or propane on Pd/γ-Al_2O_3 catalysts. *Appl. Catal. A* **2008**, *344*, 1–9.

46. Liotta, L.F. Catalytic oxidation of volatile organic compounds on supported noble metals. *Appl. Catal. B* **2010**, *100*, 403–412.

47. Avila, M.S.; Vignatti, C.I.; Apesteguía, C.R.; Garetto, T.F. Effect of support on the deep oxidation of propane and propylene on Pt-based catalysts. *Chem. Eng. J.* **2014**, *241*, 52–59.

48. Sanz, O.; Banús, E.D.; Goya, A.; Larumbe, H.; Delgado, J.J.; Monzón, A.; Montes, M. Stacked wire-mesh monoliths for VOCs combustion: Effect of the mesh-opening in the catalytic performance. *Catal. Today.* **2017**, *296*, 76–83.

49. Li, W.B.; Wang, J.X.; Gong, H. Catalytic combustion of VOCs on non-noble metal catalysts. *Catal. Today.* **2009**, *148*, 81–87.

50. Schmid, S.; Jecklin, M.C.; Zenobi, R. Degradation of volatile organic compounds in a non-thermal plasma air purifier. *Chemosphere*. **2010**, *79*, 124-130.

51. Tsai, J.H.; Chiang, H.M.; Huang, G.Y. Adsorption characteristics of acetone, chloroform and acetonitrile on sludge-derived adsorbent, commercial granular activated carbon and activated carbon fibers. *J. Haza. Mater.* **2008**, *154*, 1183-1191.